

# Atmospheric freshwater sources for eastern Pacific surface salinity

Hemerson Everaldo Tonin

M.Sc. of Physical Oceanography

University of São Paulo - Brazil

B.Sc. of Physics

University of São Paulo - Brazil

A Thesis Submitted for the Degree of Doctor of Philosophy

Flinders University

School of Chemistry, Physics & Earth Sciences

Adelaide, South Australia

2006

(Submitted October 9, 2006)

*"Something that I learned in a long life: all our science, measured against the reality, is primitive and infantile - and still thus, it is the thing more precious than we have"*

Albert Einstein

# Contents

<b>Abstract</b>	<b>xii</b>
<b>Acknowledgements</b>	<b>xv</b>
<b>1 Introduction</b>	<b>1</b>
1.1 Objectives . . . . .	11
<b>I The freshwater balance in the eastern Pacific Ocean</b>	<b>13</b>
<b>2 Literature Review</b>	<b>14</b>
<b>3 Methods and Development</b>	<b>28</b>
3.1 The role of atmospheric freshwater transport . . . . .	28
3.2 Response of the Ocean . . . . .	47
3.3 Assessment and Reflections - Part I . . . . .	62
<b>II The oceanic numerical modeling of the eastern tropical Pacific Ocean</b>	<b>78</b>
<b>4 The oceanic model</b>	<b>79</b>
4.1 Introduction . . . . .	79
4.2 The numerical ocean modeling . . . . .	81
4.3 Assessments and Reflections - Part II . . . . .	124

<b>5</b>	<b>Summary and Conclusion</b>	<b>137</b>
5.1	Introduction . . . . .	137
5.2	Synthesis of "Atmospheric freshwater sources for eastern Pacific surface salinity" . . . . .	140
5.3	Final words . . . . .	147
	<b>Bibliography</b>	<b>149</b>
<b>A</b>	<b>Statistical notes</b>	<b>165</b>
A.1	Variance . . . . .	167
A.2	Confidence intervals (CI) . . . . .	168
A.3	Empirical Orthogonal Functions (EOF) . . . . .	171
A.4	Single Value Decomposition (SVD) . . . . .	173
A.5	Wavelets . . . . .	175

# List of Figures

1.1	The Global Conveyor Belt . . . . .	3
1.2	Annual mean of the sea surface salinity of the tropical eastern Pacific and western Atlantic Ocean. (NODC (Levitus) World Ocean Atlas 1998) . .	5
1.3	A true colour image of the Inter-Tropical Convergence Zone (ITCZ) in the Central American region. . . . .	7
1.4	Schematic diagrams of oceanic and atmospheric conditions during La Niña, normal, and El Niño conditions. . . . .	9
3.1	Orthogonal planes used to establish the relationship between the atmospheric freshwater coming from Atlantic Ocean - FTr - (and/or carried out by Southerly winds along the west coast of South America - FStH) and the precipitation over the eastern Pacific Ocean. . . . .	30
3.2	Time series of the ratio of the spatially integrated atmospheric freshwater exported to the region shown in Figure 3.1 by northern hemisphere Trade Winds and spatially integrated freshwater exported to the same region region by Southerly winds along the west coast of South America (FTr/FStH). . . . .	32
3.3	Time series of spatially integrated fields, normalized by their respective standard deviation, compared by pairs. The domain of spatial integration is confined to planes defined at Figure 3.1. . . . .	35
3.4	Results of Wavelet analysis for the expansion coefficients of the first SVD mode when applied to: (a) precipitation (P), and (b) atmospheric freshwater transported by northern hemisphere Trade Wind (FTr). . . . .	41

3.5	Results of Wavelet analysis for the expansion coefficients of the second SVD mode when applied to: (a) P, and (b) FTr. . . . .	42
3.6	Results of Wavelet analysis for the expansion coefficients of the third SVD mode when applied to: (a) P, and (b) FTr. . . . .	43
3.7	Results of Wavelet analysis for the expansion coefficients of the first SVD mode when applied to: (a) precipitation (P), and (b) atmospheric freshwater transported by Southerly winds along the west coast of South America (FStH). . . . .	44
3.8	Results of Wavelet analysis for the expansion coefficients of the second SVD mode when applied to: (a) P, and (b) FStH. . . . .	45
3.9	Results of Wavelet analysis for the expansion coefficients of the third SVD mode when applied to: (a) P, and (b) FStH. . . . .	46
3.10	The proposed oceanic model domain and the TAO array of the NOAA . . . . .	48
3.11	Comparison between time series of Sea Surface Salinity (SSS) on the Equator at 140°W (a), 125°W (b), 110°W (c) and 95°W (d) as calculated by the numerical model. Result using original precipitation data from ECMWF-ERA40 ("Control Run" - Ctrl) <i>versus</i> reconstructed precipitation with variability computed from the first three SVD modes of the coupling between P and FTr with regard to the horizontal plane shown in Figure 3.1. . . . .	52
3.12	Comparison between time series of Sea Surface Salinity (SSS) on the Equator at 140°W (a), 125°W (b), 110°W (c) and 95°W (d) as calculated by the numerical model. Result using original precipitation data from ECMWF-ERA40 ("Control Run" - Ctrl) <i>versus</i> reconstructed precipitation with variability computed from the first three SVD modes of the coupling between P and FStH with regard to the horizontal plane shown in Figure 3.1. . . . .	54

3.13	The time series of the difference between the surface salinity from both independently runs ( $\Delta S = \text{SSS}(\text{FStH}) - \text{SSS}(\text{FTr})$ ) for 95°W-Equator, and its relation with ENSO cycle. . . . .	58
3.14	a) The best correlation index map (%) of the difference between the SSS from both independent runs ( $\Delta S = \text{SSS}(\text{FStH}) - \text{SSS}(\text{FTr})$ ) and ENSO cycle; b) The time lag (months) applied to the correlation analysis between $\Delta S$ and the SOI to achieve the best correlation. . . . .	60
3.15	a) The best correlation index (%) along the Equator between the signal of the salinity anomaly ( $\Delta S = \text{SSS}(\text{FStH}) - \text{SSS}(\text{FTr})$ ) and the ENSO cycle; b) Time lag along the Equator applied to achieve the respective best correlation index between $\Delta S$ and the SOI index. . . . .	61
4.1	Time series of the Sea Surface Salinity (SSS) along the Equator, for longitudes 140°W (a), 125°W (b), 110°W (c) and 95°W (d), from the numerical model and <i>in situ</i> data from TAO moored buoys. . . . .	88
4.2	Time series of salinity field volume-integrated (as output of the Ctrl) over the entire model domain and Southern Oscillation Index (SOI). . . . .	90
4.3	Time series of the depth (m) of 20°C isotherm (Z20) along the Equator, for longitudes 140°W (a), 125°W (b), 110°W (c) and 95°W (d), from the numerical model and <i>in situ</i> data from TAO moored buoys . . . . .	93
4.4	Spatial pattern and time series of the expansion coefficients of the first EOF mode of the monthly mean of the SSS . . . . .	95
4.5	Spatial pattern and time series of the expansion coefficients of the second EOF mode of the monthly mean of the SSS . . . . .	96
4.6	Spatial pattern and time series of the expansion coefficients of the third EOF mode of the monthly mean of the SSS . . . . .	96
4.7	Results of Wavelet analysis for the expansion coefficients of the first EOF mode of the SSS. . . . .	99
4.8	Results of Wavelet analysis for the expansion coefficients of the second EOF mode of the SSS. . . . .	99

4.9	Results of Wavelet analysis for the expansion coefficients of the third EOF mode of the SSS. . . . .	100
4.10	Sections of the mean zonal fields along the Equator as estimated by the Ctrl output ((a) Mean zonal velocity, (b) Mean zonal salinity, and (c) Mean zonal temperature). . . . .	102
4.11	Time-vertical-meridional average of the zonal current volume transport, as output from the Ctrl, for SEC(N), EUC, and SEC(S) in the eastern equatorial Pacific Ocean. . . . .	106
4.12	The time-averaged mean salinity field associated with the equatorial current system of the eastern Pacific Ocean as output from the Ctrl. . . . .	109
4.13	Result of wavelet when applied to the time series of expansion coefficients as a result of the first EOF mode of the zonal distribution of the mean salinity associated with the SEC(N). . . . .	113
4.14	Result of wavelet when applied to the time series of expansion coefficients as a result of the first EOF mode of the zonal distribution of the mean salinity associated with the EUC. . . . .	113
4.15	Result of wavelet when applied to the time series of expansion coefficients as a result of the first EOF mode of the zonal distribution of the mean salinity associated with the SEC(S). . . . .	114
4.16	Mean salt entrainment (PSU) into the mixed layer through its base (averaged over the entire period). . . . .	118
4.17	Temporal and spatial distribution of salt entrainment into the mixed layer from below along 95°W, for Equator and Latitudes 3°N and 3°S. . . . .	119
4.18	The correlation map between the time derivative of the Sea Surface Salinity (SSS), and the flow of atmospheric freshwater ( $E - P$ ). . . . .	122



# List of Tables

1.1	Some atmospheric phenomena which are quite well correlated with the strength of the Global Conveyor Belt . . . . .	10
3.1	Results for the first three SVD modes, when applied to the following pairs of fields jointly: a) Precipitation (P) and atmospheric freshwater transported by northern hemisphere Trade Winds (FTr); b) P and atmospheric freshwater transported by Southerly winds along the west coast of South America (FSth). . . . .	37
4.1	Results for the first three EOF modes when applied to the monthly mean of Sea Surface Salinity (SSS) as output by the Ctrl. . . . .	95
4.2	The eastern equatorial Pacific Ocean current system's definition (Johnson <i>et al.</i> , 2002b) . . . . .	104
4.3	Results of the first three main EOF modes for the zonal variation in time of the salinity field (vertical and meridional averaged) in the eastern equatorial Pacific Ocean current system. . . . .	111

# Glossary of Acronyms

ADCP	Acoustic Doppler Current Profiler
ATM	Active Tracer Model
COARE	Coupled Ocean-Atmosphere Response Experiment
COI	Cone of Influence
CTD	Conductivity-Temperature-Depth
Ctrl	Control run of the Active Tracer Model
E	Evaporation
ECMWF-ERA40	European Centre for Medium range Weather Forecasts - 40 year Re-analysis
ENSO	El Niño - Southern Oscillation
EOF	Empirical Orthogonal Functions
EPIC	Eastern Pacific Investigation Process
EUC	Equatorial Under Current
P	Precipitation
FSth	Atmospheric freshwater transported by Southerly winds along the west coast of South America
FTr	Atmospheric freshwater transported by northern hemisphere Trade Winds
GCB	Global Conveyor Belt
GCM	General Circulation Model
ITCZ	Inter-Tropical Convergence Zone
MJO	Madden Julian Oscillation
MLD	Mixing Layer Depth

MOC	Meridional Overturning Circulation
MOM	Modular Ocean Model
NADW	North Atlantic Deep Water
NAM	North American Monsoon
NAO	North Atlantic Ocean
NEC	North Equatorial Current
NECC	North Equatorial Counter Current
NOAA	National Ocean and Atmosphere Administration
NPO	North Pacific Ocean
P	Precipitation
PSU	Practical Salinity Unit
SAT	Surface Air Temperature
SEC	South Equatorial Current
SEC(N)	South Equatorial Current - North branch
SEC(S)	South Equatorial Current - South branch
SLP	Sea Level Pressure
SOI	Southern Oscillation Index
SVD	Single Value Decomposition
TAO	Tropical Atmosphere Ocean project
Z20	Depth of the 20°C isotherm

# Abstract

The remarkable salinity difference between the upper Pacific and Atlantic Oceans is often explained through net export of water vapour across Central America. To investigate this mechanism a study of salinity signals in the Equatorial Pacific Ocean current system was made looking at responses to fresh water input from two sources (local *versus* remote - Atlantic Ocean) as well as a combination of the two. Statistical analyses (Empirical Orthogonal Functions, Single Value Decomposition and Wavelet analysis) were used to split the main sources of the atmospheric freshwater input into local and remote contributions and to quantify both contributions. The remote source was assumed to have been transported over Central America from the Atlantic Ocean as an atmospheric freshwater flux, whereas the local source originated in the Pacific Ocean itself. The analysis suggests that 74% of the total variance in precipitation over the tropical eastern Pacific is due to water vapour transport from the Atlantic. It also demonstrates strong influence of ENSO events, with maximum correlation at a two months time lag. During La Niña periods the precipitation variance is more closely related to water vapour transport across Central America (the remote source), while during El Niño periods it is more closely related to the water vapour transport by Southerly winds along the west coast of South America (the local source). The current and temperature fields provided by the Modular Ocean Model (version 2) were used to study the changes in the salinity field when freshwater was added to or removed from the model. ECMWF ERA-40 data taken from the ECMWF data server was used to determine the atmospheric flux of freshwater at the ocean surface, in the form of evaporation minus precipitation (E-P). The Mixed Layer Depth (MLD) computed from temperature and salinity fields determines to what depth the salinity's

dilution/concentration takes place for every grid point. Each MLD was calculated from the results of the previous time step, and the water column was considered well mixed from the surface to this depth. The statistical relationships were used to reconstruct the precipitation over the tropical eastern Pacific. A numerical ocean model, which uses currents and temperature from a global ocean model and is forced by precipitation, was used to study the ocean's response to either the remote or the local source acting in isolation. Through time lag correlation analysis of the sea surface salinity anomalies produced by the variation in the reconstructed precipitation fields, it is found that the anomaly signals of salinity propagate westward along the Equator at a rate of approximately  $0.25 \text{ m.s}^{-1}$  (6.1 degrees per month).

"I Hemerson Everaldo Tonin, certify that this thesis does not incorporate without acknowledgment any material previously submitted for a degree or diploma in any university; and that to the best of my knowledge and belief it does not contain any material previously published or written by another person except where due reference is made in the text."

Candidate:

---

Hemerson Everaldo Tonin

# Acknowledgements

I would like to thank,

My wife Renata for the support, encouragement and patience.

My daughter Beatriz for her smile.

My family (even far, far away) in many ways have supported me.

My advisers, Prof. Matthias Tomczak and Dr. Meghan Francis Cronin my gratitude for the support, encouragement and guidance.

The Emeritus Professor Geof Lennon my gratitude for his inestimable help in the process of the revision of this document.

Dr. Gabriel Vecchi (NOAA/GFDL), Dr. D. E. Harrisson (NOAA/PMEL), Dr. Christopher Torrence (U. of Colorado) and Dr. Gilbert Compo (U. of Colorado) for valuable contributions.

Ferret analysis and visualization package developed at NOAA/PMEL (<http://ferret.wrc.noaa.gov/Ferret/>).

Mário Nantes and Yvonne Corcoran-Nantes for their friendship.

Friends and staff of the School of Chemistry, Physics & Earth Sciences at Flinders University.

Last but no least, the Brazilian Government through the CAPES Foundation by the financial support during this work.

# Chapter 1

## Introduction

The Pacific Ocean, which is the largest maritime mass on Earth, covers almost one third of the surface of the planet and corresponds to almost half of the surface and half of the volume of all the oceans. The circulation of the Pacific Ocean is seen as an extremely important component of a complex global system. Interactions between the ocean and the atmosphere, which occur on a large scale in both horizontal and vertical aspects, define respective oceanic and atmospheric environments and in turn, are modified by them. The total system is assumed to have a basic role in all the forms of life on Earth, and in particular presenting conundrums to exercise the attention of environmental scientists in recent times. Climate variability, whether it be of the past, the present or indeed of the future, must be seen to be linked to the global processes of interaction between atmosphere and ocean.

The circulation of the waters of the oceans in its broadest sense acts as the basic agent for the distribution of heat over the surface of the Earth. This affects the global climatic system as a whole. The oceanic currents are caused by the differential heating systems at different points of the Earth, by solar radiation and the resultant major wind systems. Said in another way, the general oceanic circulation responds to the effect of those processes which modify the distribution of water properties in the ocean and to the action of the winds on the surface of waters, and therefore, the oceanic currents are the joint result of the effect of the winds and the variations of buoyancy. In both cases, the displacements continue far beyond the region of their origin. Even,



when the interest is confined to a single limited area, the implication then is that there exists a need to extend the focus of attention to ever wider and distant regions together with associated observational exercises. Having this distinction in mind, the properties of the Pacific Ocean can not be seen simply as a static signature, as a result of the local regional climate, but also to have the ability to interact, influence and respond to both atmospheric processes on the one hand, and through changing buoyancy, to the three-dimensional structure of the ocean on the other. It is against this background that a search is conducted here for evidence and for an explanation of the interactive processes which determine the water properties of the tropical eastern Pacific, and the resultant links with climate.

In this context, one of the most characteristic aspects of global oceanic circulation under the present ocean circulation is the so-called Global Conveyor Belt (Gordon, 1986). A key feature is that it delivers an enormous amount of heat to the North Atlantic. Norway, at  $60^{\circ}\text{N}$  is far warmer than southern Greenland or northern Labrador at the same latitude. Palm trees grow on the west coast of Ireland, but not in Newfoundland which is further south. The thermohaline circulation does have a significant impact, warming Western Europe by about  $5^{\circ}\text{C}$  relative to the similarly located west coast of Canada. An oversimplified schematic diagram of the Global Conveyor Belt (Broecker, 1991) is shown in Figure 1.1. Since the conveyor forms a closed loop, a description of it can begin anywhere, but actually the density function of the temperature and the salinity of the ocean water as it responds to a relative anomaly of buoyancy with respect to ambient water properties, having moved to a new environment, determines the onset and maintenance of this type of circulation. The thermohaline circulation, as its name indicates, is generated by the variations of temperature and salinity, of, say, a warm water body transported poleward into cooler climes, and thereby exposed to cooling and a loss of buoyancy with respect to its new neighborhood. If unaffected by atmospheric exposure to fresh water precipitation, such a water body might well be subjected to downward convection to a level of similar buoyancy and thence to a

subsurface return to lower latitudes. Meanwhile of course the system would be affected by the interplay of atmospheric influences applied to the surface, which might include reduction of the body's salinity due to precipitation, further increasing its buoyancy, or perhaps the reverse due to excessive evaporation which would increase salinity and mitigate against the above convection. Nevertheless such downward convective processes have an innate ability to drive a poleward flow of heat at the surface.

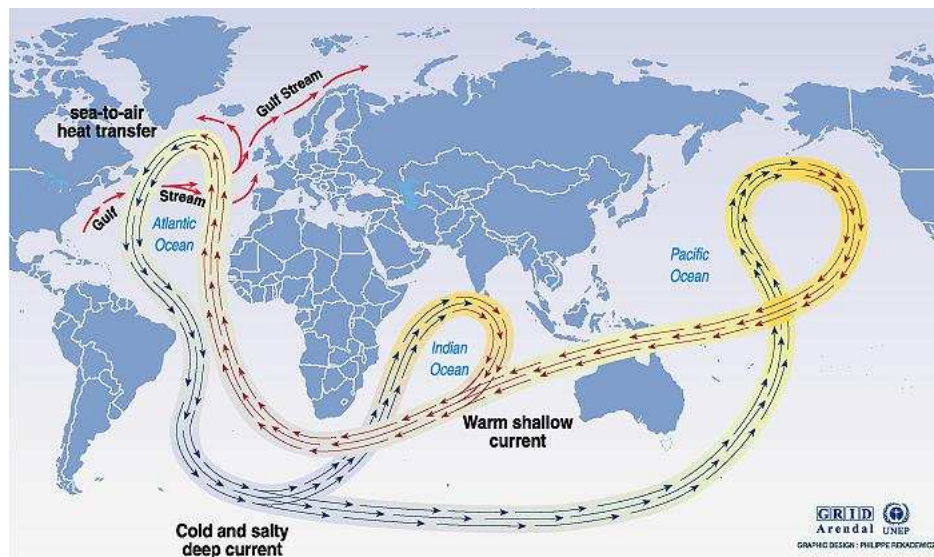


Figure 1.1: The Global Conveyor Belt (*Source: Broecker, 1991. In: Climate change 1995, Impacts, adaptations and mitigation of climate change: scientific-technical analyses, contribution of working group 2 to the second assessment report of intergovernmental panel of climate change. UNEP and WMO. Cambridge University Press, 1996 - 30/Jun/2006*)

The motor force of the thermohaline circulation is the formation of the water masses. These water masses are characterized by well defined salinity and temperatures and are created in specific regions of the oceans by surface processes. Such physical attributes as temperature and salinity define a property that characterizes and specifies this water mass: its density, which is a defining characteristic during its displacement

in the oceans. Currents then carry the water to other parts of the ocean. At all times, the water parcel moves in accordance with the maintenance of the relative buoyancy in its vicinity.

There are two main processes of formation of water masses: the deep convection described above and the subduction while both are related to the dynamics of the mixed layer in the surface of the ocean. The formation of water masses by subduction occurs mainly in the subtropical regions, where the water at the bottom of the mixing layer is pumped further downwards by the convergence formed in the Ekman transport and which descends slowly through levels of constant density within that water mass. The other mechanism of formation of deep water masses - the convective method - occurs in regions with little stratification of density, and its precondition for formation is that during winter, cold water formed at the surface sinks to a depth determined by its density, relative to the density of the under-lying water. Deep water formation through major downward convection is not observed in the Pacific Ocean. The Pacific Ocean, especially in the north, is too fresh by comparison with the northern Atlantic Ocean, even though both northern oceans have approximately the same sea surface temperature. The surface waters of the Pacific lack the salinity of their Atlantic counterparts, and consequently do not display sufficient water density to drive the downward convection as in the Atlantic. This remarkable salinity difference between the Pacific and Atlantic Oceans is one of the most noticeable features of the global upper ocean (Figure 1.2). The Pacific Ocean is about two salinity units fresher than the Atlantic Ocean, and this has earlier been mentioned to explain why no deep water is produced in the Pacific (Warren, 1983).

The striking salinity difference between the Pacific and Atlantic oceans has traditionally been explained by an atmospheric net freshwater transport across the Central American land bridge (Dietrich *et al.*, 1980). As they traverse the subtropical oceans, the Trade Winds become saturated with moisture, which is released as oro-

ographic rain as the winds encounter the mountain chains of the continents. In Central America, the mountain chain is broken by gaps, and the narrowness of the land bridge allows much of the orographic rain to reach the tropical eastern Pacific, causing a large difference in sea surface salinity between the near-adjacent Pacific and Atlantic coast zones of Central America.

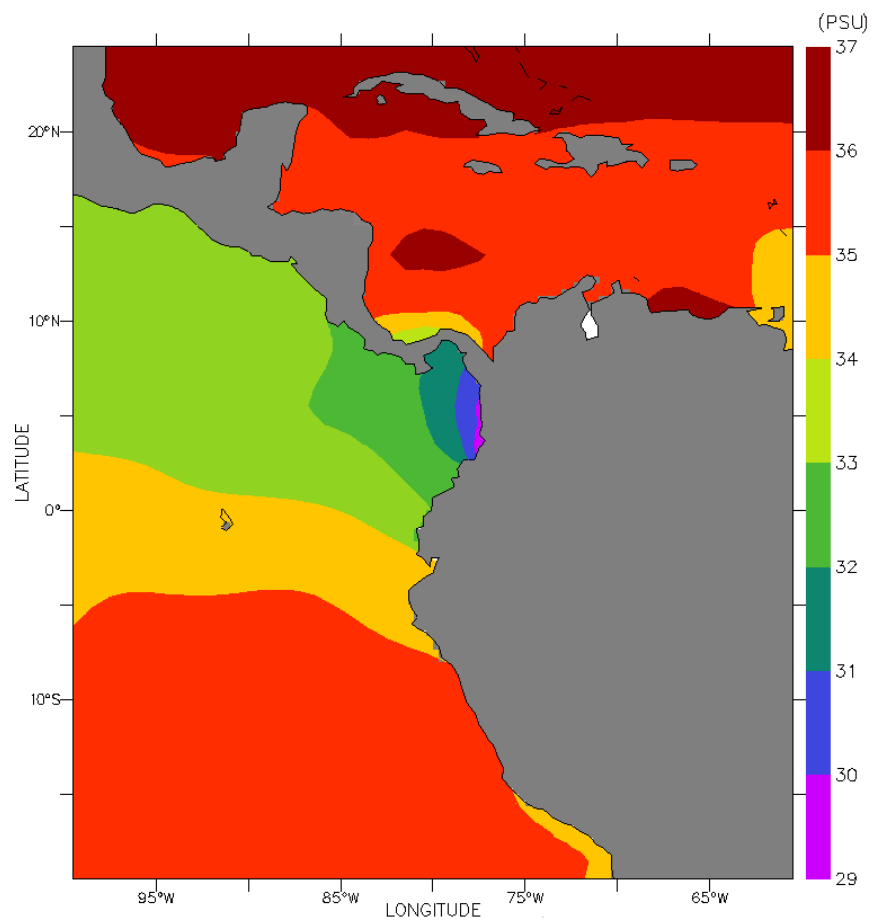


Figure 1.2: Annual mean of the sea surface salinity (in PSU - Practical Salinity Units) of the tropical eastern Pacific and western Atlantic Ocean (*adapted from*: NODC (Levitus) - World Ocean Atlas 1998 <<http://www.cdc.noaa.gov>> - 30/Jun/2006)

An endeavour to unify the two remarkable characteristics of the oceans: - the Global Conveyor Belt (GCB) in relation to the global oceanic current system, and the striking salinity difference between Pacific and Atlantic oceans - was attempted by Broecker (1991). His study suggests that the GCB is driven by the atmospheric transport of water vapour from the Atlantic basin to the Pacific - water evaporating from the Atlantic and precipitation as rain in the Pacific catchments. His theory relies on the strength of the conveyor belt flow to be proportional to the water vapour transport: water evaporating from the Atlantic leaves the salt behind, and it falls down as rainfall, diluting the Pacific and at the same time maintaining a saltier Atlantic Ocean. In this manner downward convection is inhibited in the northern Pacific but strengthened in the northern Atlantic.

Another factor which must be considered with regard to the freshness of the Pacific Ocean, more specifically in relation to its eastern tropical region is the role of the Inter-Tropical Convergence Zone. The Inter-Tropical Convergence Zone (ITCZ) is the region between the southern and northern hemisphere Trade Winds, where upward air movement causes the moisture to condense into clouds (Figure 1.3). As the air rises, it cools, releasing the accumulated moisture in an almost perpetual series of thunderstorms. Weather stations in the equatorial region experience precipitation for up to 200 days each year, making the region under the ITCZ the wettest on the planet. Net precipitation minus evaporation (P-E) exceeds 2.5 m/year in the Pacific ITCZ everywhere, in contrast to values closer to 1.5 m/year elsewhere (Oberhuber, 1988). Such large amounts of freshwater must leave their imprint on the sea surface salinity. But the question remains: how much of the moisture that condenses into rain in the Pacific ITCZ evaporated originally from the Atlantic Ocean?



Figure 1.3: A true colour image of the Inter-Tropical Convergence Zone (ITCZ) in the Central American region. Clouds form along region of wind convergence, where rising air causes condensation and eventually rainfall. (*clipped from:* <[http://earthobservatory.nasa.gov/Newsroom/NewImages/Images/Images/itcz\\_goes11\\_lrg.jpg](http://earthobservatory.nasa.gov/Newsroom/NewImages/Images/Images/itcz_goes11_lrg.jpg)> - 30/Jun/2006).

---

An important factor known to influence ITCZ rainfall over the tropical eastern Pacific is the status of the Walker Circulation. This entirely ocean-based zonal atmospheric circulation cell comes about as the result of a marked difference in the surface temperatures of the western and eastern Pacific Ocean. When the western Pacific waters are warm and the eastern waters are cool, strong convective activity over equatorial East Asia and subsiding cool air off South America's west coast create a wind pattern that pushes surface water westward and raises surface levels in the western Pacific. When the atmospheric convective activity in the western Pacific abates, this circulation is broken. Initially, the upper-level westerly winds fail. This cuts off the source of cool subsiding air and therefore the surface easterlies cease. As a consequence, in the eastern Pacific warm water surges in from the west, since the surface wind which acted to constrain it is weakened. This produces long-term unseasonable temperatures and precipitation patterns in Central, North and South America as well as in Australia and south east Africa, and disruption of ocean currents.

The above described phenomenon, known as the El Niño-Southern Oscillation (ENSO), is closely related to instability of the tropical Pacific ocean-atmospheric system. ENSO is the most prominent known source of inter-annual variability in weather and climate around the world ( $\sim 3$  to 8 years), though not all areas are affected. The knowledge of conditions in the tropical Pacific is considered essential for the prediction of climate variations for both short-term and long-term, and therefore, ENSO has attracted much attention since the 1980's (Philander *et al.*, 1984). The opposite of an El Niño event is known as a La Niña. In this case, the convective cell over the western Pacific strengthens inordinately, resulting in colder than normal winters in North America, with a more robust hurricane season in South-East Asia and Eastern Australia. There is increased upwelling of deep cold ocean waters and more intense uprise of surface air near South America, resulting in increasing numbers of drought occurrence, although it is often argued that fishermen reap benefits from the more nutrient-filled eastern Pacific waters. Figure 1.4 shows schematic diagrams of oceanic and atmospheric conditions during a typical La Niña - which is characterized by a strong Walker circulation (left panel), for normal conditions (central panel), and for El Niño conditions (right panel) - when the Walker circulation weakens or reverses. While the Walker circulation (east-west atmospheric circulation) decreases in intensity, the intensity of the Hadley circulation (north-south atmospheric circulation) increases due to enhanced equator-pole gradient, influencing weather at higher latitudes. The Hadley circulation is a closed circulation loop, which begins at the Equator with warm, moist air lifted aloft in equatorial low pressure areas to the tropopause then carried poleward. At about  $30^{\circ}\text{N/S}$  latitude, it descends in a cooler high pressure area. Some of the descending air travels equatorially along the surface, closing the loop of the Hadley cell and creating the Trade Winds. These winds are not nearly as strong as those aloft.

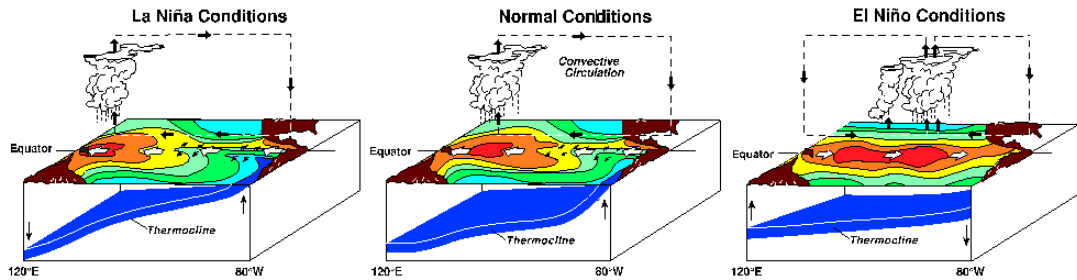


Figure 1.4: Schematic diagrams of oceanic and atmospheric conditions during La Niña conditions (left panel), normal conditions (central panel), and El Niño conditions (right panel). The atmospheric features show the changes in the Walker circulation and as a consequence, the longitudinal shift of the position of the precipitation zone in the equatorial Pacific Ocean, while that the oceanic conditions show their implications in thermocline. (<[http://www.pmel.noaa.gov/tao/el\\_nino/nino-home.html](http://www.pmel.noaa.gov/tao/el_nino/nino-home.html)> - 30/Jun/2006)

Gray, an American meteorologist, has suggested links between the Global Conveyor Belt and climate over the past 125 years. He identified four distinct periods, two when the conveyor belt was very active, two when it was quite inactive. He also found several important atmospheric phenomena which correlate quite well with the strength of the conveyor (Gray, 1984a, b; Taylor, 1995). When the conveyor flows strongly there is an increase in the number of hurricanes, heavy rainfall in the Sahel region along the southern edge of the Sahara Desert, few ENSO events, and a general decrease in global mean temperatures. These conditions occurred between 1870 and 1899, and between 1943 and 1967. When the conveyor flows weakly, as it did between 1900 and 1942, and again between 1968 and 1993, there are fewer hurricanes and more ENSO events, rainfall in the Sahel region is average or below average, and global mean temperatures are higher. Some scientists fear that a general increase in global temperatures may affect the formation of North Atlantic Deep Water (NADW) and trigger a change in the conveyor, causing it to flow more weakly or even to shut down. Were this to happen, it is possible that global warming might induce ice age conditions in northern Europe. An updated of some atmospheric phenomena which are quite well correlated



with the strength of the Global Conveyor Belt based on the Gray's suggestions can be summarized in the following table (Table 1.1).

---

Table 1.1: Some atmospheric phenomena which are quite well correlated with the strength of the Global Conveyor Belt - analyses for the period of 125 years, finishing in 1993 ( *adapted from:* <<http://www.ocs.orst.edu/reports/conveyor.html>> - 13/Jun/2006)

---

<b>Parameter</b>	<b>1870-1899</b>	<b>1900-1942</b>	<b>1943-1967</b>	<b>1968-1993</b>
Conveyor belt	Strong	Weak	Strong	Weak
Atlantic hurricane activity	Enhanced	Suppressed	Very enhanced	Somewhat suppressed
Sahel rainfall	Very wet	Average	Very wet	Very dry
El Niño events	Few	Many	Few	Many
Global air temperatures	Decrease	Increase	Decrease	Increase

---

At last, the physical and dynamic processes in the ocean and in the atmosphere are seen to form an integrated system, and not a series of random events. The processes of interaction seem to follow a circuit of cause and effect, where an alteration in one of them has a consequence in the other.

## 1.1 Objectives

The intention in the work which follows is to accept the above concepts of interaction between atmosphere and ocean on a global scale and to focus particularly on the basic anomaly between the tropical Atlantic and the tropical Pacific which is becoming increasingly clear to be an important contributor to the driving forces of the GCB. The objective then is to clarify and confirm the role of this inter-ocean anomaly in the global picture and to harness new contenders and techniques which may unravel the total mechanism.

This study then is focused on the eastern Pacific Ocean. A combination of numerical modeling, observations and statistical analyses are employed on the one hand to quantify the role of moisture transport from the Atlantic together with condensation and rainfall in the ITCZ, on the other hand to investigate then modulation of both processes by the ENSO. The sea surface salinity is to be used as a tracer of the results. The atmospheric part of this study is based on reanalysis data, and its oceanic counterpart on both a general ocean circulation model and a mixed layer model.

Although this study is mainly focused on the atmosphere, the sea surface salinity plays a major role as a tracer of the atmospheric alterations, and consequently, the features of the sea surface salinity, in some form, are considered as of those atmospheric changes. The western Pacific Ocean has been studied extensively in recent years, basically with respect to the function of the warm pool and its implications for the El Niño-La Niña system. The focus to date has invariably been on the tropical western Pacific. The intention here is to redress this balance and to direct attention to the mechanisms affecting the eastern tropical Pacific as these arguably have the potential to control the wider global ocean circulation at a more fundamental level. Thus, the considerable absence of recent specific literature in relation to some aspects of the eastern Pacific gives an extra relevance to the oceanic numerical model.

In summary, the study is divided into two parts, with specific objectives as follows:

**Part I - The freshwater balance in the eastern Pacific Ocean**

- To establish the role of atmospheric freshwater transported by northern hemisphere Trade Winds, and by Southerly winds along the west coast of South America in the precipitation over the eastern Pacific Ocean, then to examine their mix in contributing to precipitation in the eastern tropical Pacific;
- To investigate their temporal variability associated with ENSO;
- To quantify their implications for the surface salinity of the eastern tropical Pacific Ocean.

**Part II - The oceanic numerical modeling of the eastern tropical Pacific Ocean**

- To construct and validate a reliable oceanic numerical model in which a prescribed atmospheric freshwater flux provides an independent input parameter;
- To examine the salinity field through complementary analyses, searching for a better understanding of certain aspects of this property in the eastern tropical Pacific Ocean.

The fundamental objective is to clarify the main mechanisms which control the anomalous salinity properties of the adjacent Pacific and Atlantic Oceans with particular reference to the latitudes of the Central American Isthmus. The aim is to investigate the source of this anomaly. It is anticipated that such an approach may also provide a complementary tool to help to elucidate components of the interactive role of Global Ocean and Global Atmosphere, ultimately approaching the modern enigmas of climate change and climate variability.